Molecular line parameters for the MIPAS (Michelson Interferometer for Passive Atmospheric Sounding) experiment

J.-M. Flaud,[1] C. Piccolo,[2] B. Carli,[2] A. Perrin,[1] L.H. Coudert,[1] J.-L. Teffo,[3] and L.R. Brown[4]

[1] *Laboratoire de Photophysique Moleculaire, CNRS, Université de Paris Sud, France*
[2] *IFAC-CNR Firenze, Italy*
[3] *Laboratoire de Physique Moleculaire et Applications, CNRS, Université P. et M. Curie, France*
[4] *California Institute of Technology, Jet Propulsion Laboratory, Pasadena, California, USA*

Received January 16, 2003

The Michelson Interferometer for Passive Atmospheric Sounding (MIPAS) experiment is operating on board the ENVISAT satellite and uses a Fourier-transform spectrometer to acquire for the first time high spectral resolution middle infrared emission limb sounding spectra of the Earth atmosphere from space. The measurement capabilities make it possible to determine every 75 s the vertical profile of several atmospheric trace constituents, during both day and night with an almost full coverage of the globe. This leads to a three dimensional measurement of the atmospheric composition. In order to handle the large data flow, an optimized code for the Level 2 near real time analysis of MIPAS data was developed by an international consortium of scientists under an ESA contract. The code is designed to provide, in an automated and continuous mode, atmospheric vertical profiles of temperature and pressure, as well as of concentrations of O_3, H_2O, CH_4, HNO_3, N_2O, and NO_2, in the altitude range from 6 to 68 km. The analysis and interpretation of the limb spectra require good knowledge of the molecular parameters of these species as well as of the interfering species. This paper describes the spectroscopic line parameters database compiled for the MIPAS experiment.

Introduction

The Michelson Interferometer for Passive Atmospheric Sounding (MIPAS) experiment, which was switched-on on March 11th, 2002 records middle infrared emission limb sounding spectra of the Earth atmosphere at a high spectral resolution (0.025 cm^{-1} unapodized) using five spectral bands covering the spectral range 685–2410 cm^{-1}. It performs measurements in a continuous mode during both day and night, providing an almost full coverage of the globe. The analysis of each limb scanning sequence allows determining the vertical profile of several atmospheric constituents, as well as the temperature and pressure profiles. For each orbit MIPAS performs 75 scans (plus the ones used for the instrument calibration). Combining the results obtained for the scans of each orbit, the global distribution (as a function of altitude and latitude) of the geophysical parameters can be determined.

The handling of such a large flow of data requires an automated process able to perform a Near Real Time (NRT) analysis. To this purpose, an optimized algorithm, called Optimized Retrieval Model (ORM), has been developed[1] under an ESA contract by an international consortium of scientists and has been implemented in the ENVISAT Ground Segment. The code is designed to retrieve, starting from the calibrated spectra provided by Level 1B processor, atmospheric vertical profiles of temperature, tangent pressure, i.e., the value of pressure corresponding to the tangent altitude of the limb measurement, and the Volume Mixing Ratio (VMR) of 6 target species (O_3, H_2O, CH_4, HNO_3, N_2O, NO_2). For this purpose, the retrievals are performed in a set of narrow (less than 3 cm^{-1} width) spectral intervals, called "microwindows,"[2] that have been selected as those intervals which contain the best information on the target parameters and are less affected by systematic errors, such as, for instance, uncertain spectroscopic data, interference of non-target species, Non-Local Thermal Equilibrium (NLTE),[3] and line mixing effects.

Since the quality of the retrievals depends on the accuracy of the molecular line parameters, compilations of parameters were initiated and updated,[4,5] these compilations including generally for each transition the line position, the line intensity, the air-broadening coefficient (Half Width at Half Maximum (HWHM)), the self-broadening coefficient, the lower state energy, the temperature dependence of the air-broadening coefficient, the air-pressure shift, the vibrational and rotational assignments, and indices giving error estimates, and relevant literature data. The parameters are usually based on spectroscopic studies published in the open literature and are updated every two to four years. To meet in a faster way the needs of the MIPAS experiment, it was decided to generate a dedicated compilation covering the spectral domain 600–2500 cm^{-1}. This compilation was based on the HITRAN[4] and GEISA[5] databases and contains updates

0235-6880 / 03 / 03 172-11 $02.00

of existing parameters derived either from specific spectroscopic studies or from spectroscopic studies prior to their publications.

At the beginning, in absence of MIPAS measurements, measurements obtained by the Space Shuttle instrument ATMOS (Atmospheric Trace Molecule Spectroscopy)[6] were used to characterize possible spectroscopic errors and to check and validate the updates. ATMOS supplied indeed the most accurate atmospheric measurements available from satellite at limb geometry before the launch of Envisat. It is a solar occultation experiment which has an analogous satellite geometry but higher signal to noise ratio and higher resolution than MIPAS. Later on preliminary MIPAS results were also used to check the spectroscopic parameters. The bulk of the efforts were devoted to the improvement of the spectral line parameters of CO_2 (temperature and pressure retrievals) and of the 6 target species (O_3, H_2O, CH_4, HNO_3, N_2O, NO_2) but whenever possible improved line parameters for other species were also included. Finally, it is worth noticing that the format of the database as well as the numbering of the molecules and of the isotopic species is the same as in HITRAN-96 and HITRAN-2K.

Changes in molecular line parameters

This section discusses, molecule by molecule, the modifications made to the HITRAN and GEISA databases to create the MIPAS database giving arguments sustaining the updates.

1. Water vapor H_2O

In the study, three sets of spectral parameters were taken into account for the H_2O molecule (in the following, unless the isotopic species is clearly specified, the "H_2O molecule" means the various isotopic variants of this molecule, namely, $H_2{}^{16}O$, $H_2{}^{18}O$, $H_2{}^{17}O$, $HD^{16}O$, $HD^{18}O$, and $HD^{17}O$). They are:

- the HITRAN-96[4] parameters denoted in the following as 01_HIT96;
- the updated parameters which can be found on the HITRAN website[7] and which are denoted in the following as 01_HIT01;
- the parameters derived for the main isotope from recent calculations based on a new theoretical model[8–10] used to fit experimental data,[11–17] and denoted in the following as 01_CAL02.

The first step was to compare for all the isotopic species except $H_2{}^{16}O$ the spectral parameters included in the files 01_HIT01 and 01_HIT96. The results are gathered in Table 1 and one can make the following comments:

– On the average, there is a rather good agreement between the two sets of data for the strongest band ν_2 (HIT 2–1).* This is also true to a lesser extent for the weaker bands $2\nu_2 - \nu_2$ (HIT 3–2) and $\nu_3 - \nu_2$ (HIT 5–2).

– The main differences ($\cong \pm 20\%$) exist for the pure rotational band (HIT 1–1) but it should be noted that, in the spectral region that we are considering, this band is rather weak and, also considering the abundance of the various isotopic species, it is unlikely that the corresponding lines will be clearly seen in the MIPAS spectra in the stratosphere.

Table 1. Comparison of the line intensities included in the files 01_HIT01 and 01_HIT96 for the less abundant water isotopic variants (spectral domain 600–2500 cm^{-1})

Band HITRAN notation	Isotopic species				
	$H_2{}^{18}O$	$H_2{}^{17}O$	$HD^{16}O$	$HD^{18}O$	$HD^{17}O$
1–1	1.176(86) (104)	1.163(47) (65)	0.748(64) (17)	–	–
2–2					
2–1	0.997(54) (968)	0.969(46) (840)	0.984(240) (1542)	–	–
3–2	1.044(200) (262)	1.017(54) (190)	–	–	–
4–2					
5–2	1.084(48) (16)	–	–	–	–
6–3					
N(01_HIT01)	1599	1118	2355	438	175
N(01_HIT96)	1350	1148	1773	0	0

We give for each isotope and for each band the average ratio of the intensities (01_HIT01/01_HIT96), the corresponding standard deviation, and the number of lines in common (below in parenthesis). N(01_HITxx) gives for each isotope the number of lines included in the file 01_HITxx.

Given the fact that the new data are the end product of precise laboratory studies performed in recent years,[18] for all the isotopic species except $H_2{}^{16}O$ we have used these new data in the MIPAS database.

The second step was devoted to the comparison of the line intensities of the $H_2{}^{16}O$ isotopic species. The three sets of data 01_HIT96, 01_HIT01, and 01_CAL02 were compared and the results are given in Table 2.

Such comparisons were performed:

– for all pairs of common lines,

– for a pair of common lines with intensities larger than 10^{-25} $cm^{-1}/(mol \cdot cm^{-2})$, this value, while somewhat arbitrary, being considered as a lower limit for significantly absorbing lines in atmospheric spectra.

Concentrating on the strong and medium intensities (intensities larger than 10^{-25} $cm^{-1}/(mol \cdot cm^{-2})$), one can draw the following conclusions:

- For all the bands there is an excellent agreement between the 01_CAL02 and 01_HIT01 data sets.
- Whereas there is a good agreement between 01_CAL02, 01_HIT01, and 01_HIT96 for the strong band ν_2 (HIT 2–1) and for the medium hot band $2\nu_2 - \nu_2$ (HIT 3–2), 01_HIT96 shows for the other bands larger discrepancies from the other two data sets (between –5% and +20% depending on the band). As far as MIPAS is concerned such effects should be sensitive in the 14–9 μm spectral region where the pure rotational band (HIT 1–1) appears to be about 8–9% too weak in 01_HIT96.

* HITm–n is used throughout the paper to represent the vibrational assignment of a band in the HITRAN-96 notation.

Table 2. Comparison of the line intensities included in the three files 01_CAL02, 01_HIT01, and 01_HIT96 for the $H_2{}^{16}O$ molecule (spectral domain 600–2500 cm^{-1})

Band	01_HIT01 / 01_HIT96		01_CAL02 / 01_HIT96		01_CAL02 / 01_HIT01	
	$I \geq 10^{-25}$	All lines	$I \geq 10^{-25}$	All lines	$I \geq 10^{-25}$	All lines
1–1	1.093(274) (253)	1.541(1571) (463)	1.084(276) (252)	1.709(1960) (491)	0.987(58) (252)	1.063(823) (461)
2–2	0.937(40) (35)	0.958(97) (84)	0.956(40) (34)	0.906(110) (92)	1.026(51) (36)	0.955(125) (118)
2–1	1.023(97) (1286)	1.351(2466) (1671)	1.021(121) (1288)	1.387(3059) (1671)	0.998(64) (1288)	1.021(352) (1796)
3–2	1.020(125) (483)	1.100(364) (724)	1.012(109) (491)	1.084(450) (728)	0.993(73) (491)	1.014(788) (861)
4–2	1.170(289) (188)	1.437(942) (395)	1.201(289) (186)	1.322(743) (399)	1.013(120) (186)	1.088(878) (510)
5–2	1.081(133) (173)	1.099(265) (350)	1.117(137) (169)	1.236(445) (350)	1.034(66) (169)	1.178(432) (434)
6–3	0.640(255) (22)	0.871(433) (121)	–	–	–	–

We give for each band the average ratio of the intensities, the corresponding standard deviation, and the number of line in common (below in parenthesis). $I \geq 10^{-25}$ means that only lines with intensity larger than 10^{-25} $cm^{-1}/(mol \cdot cm^{-2})$ were compared.

Considering now the comparisons made when including all the lines it appears that:

- The agreement is still very good on the average for all bands when comparing 01_CAL02 and 01_HIT01 but it is worth noticing the increase of the standard deviations: this means that for the weak lines there are stronger differences.
- On the contrary both the comparison between 01_HIT01 and 01_HIT96 and the comparison between 01_CAL02 and 01_HIT96 show *i*) a strong change of the average ratios as compared to the ones obtained with the strong and medium intensities and *ii*) a strong increase in the standard deviation. All this means that very strong differences exist between the weak lines.

Given the fact that:

– as already said, the 01_HIT01 data set is based on a number of precise recent laboratory studies[18];

– the 01_CAL02 file was generated using a theoretical model[8–10] which treats simultaneously all the bands (this insures that on a relative basis the intensities are much more consistent than when a band per band treatment is used);

– the comparisons made in Table 2 show a much better agreement of 01_CAL02 with 01_HIT01 than with 01_HIT96, one can certainly conclude that the two files 01_CAL02 and 01_HIT01 provide better spectral parameters for $H_2{}^{16}O$ than 01_HIT96.

This was confirmed by a simulation of ATMOS spectra comparing 01_HIT96 and 01_HIT01 data.

Having established that 01_HIT01 and 01_CAL02 provided better spectral parameters than 01_HIT96, we modeled ATMOS spectra using 01_HIT01 and 01_CAL02. Table 3 gives a statistical analysis of the results for the $H_2{}^{16}O$ bands at a tangent altitude of 23 km. The statistics was made for 3 cm^{-1} wide intervals covering the spectral MIPAS bands, excluding those regions in which the observed ATMOS spectra were opaque and in which the effect of atmospheric continuum was significant. For each spectral band three columns are given. The first column shows the spectral intervals of the band in which the statistics was performed, the second column shows the RMS of residuals using the two different sets of data, and the third column shows the number of intervals, where the new data (in this case 01_CAL02 data) give better results, compared with the total number of intervals. Except the results in band AB and B in which the overall RMS of the residuals are comparable, considering the other bands and the total effect, and remembering that the 01_CAL02 data are consistent from a spectroscopic point of view since they result from global fits, one can conclude that there is some indication that the 01_CAL02 data set is likely to give better results than 01_HIT01.

Table 3. Comparison of simulated and observed ATMOS spectra using 01_CAL02 and 01_HIT01 data for the $H_2{}^{16}O$ molecule at 23 km

Band	Spectral domain, cm^{-1}	RMS · 10^{-2} 01_CAL02 / 01_HIT01	Number of intervals where CAL02 give better results
A	745–970	2.3581 / 2.4941	45 of 75
AB	1041–1170	1.9230 / 1.9229	16 of 38
B	1215–1500	2.2379 / 2.2357	29 of 91
C	1573–1750	2.6402 / 2.6583	32 of 59
D	1820–2240	1.8160 / 1.8444	85 of 160
Total		2.1275 / 2.1644	207 of 423

As a conclusion the H_2O line parameters included in the MIPAS database are:

– for all isotopic variants of H_2O except $H_2{}^{16}O$ the line parameters of 01_HIT01;

– for $H_2{}^{16}O$ the line parameters of 01_CAL02. It is worth noticing that these new data, which are summarized in Table 4, include also the pure rotational bands in the excited states $2\nu_2$, ν_1, and ν_3 (bands 3–3, 4–4, and 5–5 in HITRAN notation) which do not exist in the other databases;

– for the band HIT 6–3 of the main isotope the data from 01_HIT01 were kept.

Table 4. Summary of the $H_2{}^{16}O$ bands coming from 01_CAL02 included in the MIPAS database (spectral domain 600$2500 cm$^{$1}$)

#	Band	XMIN	XMAX	SMIN	SMAX	STOT	NB
1	0 0 0 0 0 0	600.0273	1457.6674	0.101D$26	0.248D$20	0.224D$19	506
2	0 0 1 0 2 0	600.8882	913.0041	0.101D$26	0.838D$25	0.112D$23	78
3	0 2 0 0 2 0	601.0321	645.1868	0.137D$26	0.466D$26	0.803D$26	3
4	0 1 0 0 1 0	601.5922	1883.9023	0.100D$26	0.326D$23	0.215D$22	152
5	1 0 0 0 2 0	634.2877	829.0096	0.124D$26	0.514D$26	0.270D$25	11
6	0 1 0 0 0 0	640.5014	2497.2495	0.100D$26	0.314D$18	0.111D$16	1928
7	0 2 0 0 1 0	819.7767	2406.1835	0.103D$26	0.277D$21	0.953D$20	971
8	1 0 0 0 1 0	1221.4098	2496.8647	0.101D$26	0.377D$23	0.150D$21	624
9	0 0 1 0 1 0	1298.1170	2497.6887	0.103D$26	0.915D$23	0.234D$21	477
10	0 2 0 0 0 0	2387.9933	2449.9804	0.256D$26	0.718D$26	0.975D$26	2

The meaning of the different columns is: Band: Vibrational assignment; XMIN, XMAX: Minimum and maximum line positions SMIN, SMAX: Minimum and maximum line intensities; STOT: Total band intensity; NB: Number of lines.

2. Carbon dioxide CO_2

The most recent version of the HITRAN database, HITRAN-2K, includes for carbon dioxide the same spectral parameters as HITRAN-96.[4] These data were mainly derived using the DND (Direct Numerical Diagonalization) method.[19] However, more recently an analogous method based on global fits of observed frequencies and line intensities using the effective operator approach[20–27] was developed and used to generate new line parameters (Carbon Dioxide Spectroscopic Databank or CDSD) for the four most abundant isotopic species of carbon dioxide, namely, $^{12}C^{16}O_2$, $^{13}C^{16}O_2$, $^{16}O^{12}C^{18}O$, and $^{16}O^{12}C^{17}O$. As for water vapor we have first made a summary of all the bands included in the new CDSD data together with the same information for the HITRAN data and have compared them.

The first remark concerns the fact that both the numbers of bands and lines are larger for the CDSD than for HITRAN showing that the former database is more extensive and includes bands which are not included in HITRAN. However it should be noticed that generally the new bands are rather weak.

To go further, we have compared the intensity ratios of all the lines common to the two databases. One can make the following comments:

– As already stressed a number of bands are present in CDSD and not in HITRAN.

– For the majority of bands the ratios are not very different from 1 with a small standard deviation. In these cases it is clear that the two databases are in satisfactory agreement.

– For some bands the ratios are not far from unity but the standard deviation is no longer small. This proves that there is a discrepancy between the two databases: For example the *R*-lines exhibit a ratio larger than 1, while the *P*-lines lead to a ratio smaller than 1, the average being around 1.

– Finally for some bands the average ratio is no longer equal to 1 showing a clear disagreement.

Having demonstrated that the two databases are different, it proved the necessity of checking them by simulating, as for H_2O, ATMOS spectra and making comparisons.

The comparisons with the ATMOS spectra were performed for three tangent altitudes, namely, 15, 27, and 43 km to see the effects in the change for the weak, medium and strong lines and using on the one hand the HITRAN database and on the other hand the CDSD complemented by the HITRAN line parameters for the isotopomers of CO_2 not accounted for in CDSD.

The results of the simulation of the ATMOS spectra are shown in Table 5 where a statistical analysis of the residuals was performed. As in the case of the analysis of water vapor, the statistics was made for 3 cm^{-1} wide intervals covering the spectral MIPAS bands, excluding those regions in which the observed ATMOS spectra were opaque and in which the effect of atmospheric continuum was significant. For each spectral band three columns are given. The first column shows the spectral intervals of the band in which the statistics was performed, the second column shows the RMS of residuals using the two different sets of data, and the third column shows the number of intervals, where the new data (in this case CDSD) give better results, compared with the total number of intervals.

Table 5. Comparison of simulated and observed ATMOS spectra using CDSD and HITRAN-2K

Band	Spectral domain, cm^{-1}	RMS · 10^{-2} CDSD / HITRAN-2K	Number of intervals where CDSD give better results
		15 km	
A	925–971	4.62240 / 4.6593	13 of 16
AB	1065–1092; 1122–1170	–	$
B	1215–1278; 1310–1500	2.5182 / 2.5157	18 of 34
D	1820–2102; 2111–2201	2.5057 / 2.5026	24 of 64
Total		2.8065 / 28092	55 of 114
		27 km	
A	704–752; 826–971	2.6664 / 2.6561	23 of 47
AB	1065–1092; 1122–1170	1.3784 / 1.3800	8 of 30
B	1215–1278; 1310–1500	2.1366 / 2.1354	24 of 55
D	1820–2102; 2111–2201	1.8282 / 1.8545	71 of 136
Total		1.9877 / 1.9996	126 of 268
		43 km	
A	680–770; 925–971	2.9032 / 2.9033	19 of 45
AB	1065–1092; 1122–1170	1.4803 / 1.4806	21 of 49
B	1215–1278; 1310–1500	1.1645 / 1.1647	10 of 19
D	1820–2102; 2111–2201	1.4624 / 1.7548	81 of 128
Total		1.7116 / 1.8670	131 of 241

From this comparison it appears that, even if the percentage of intervals in which the new data are better is not decisive, the overall RMS in all bands together is better with the new data (CDSD) than with the HITRAN data. A more detailed analysis shows that it is somewhat difficult to discriminate between the two sets of data except for band D for which the new set gives significantly better agreement.

Having established the fact that the CDSD is consistent, from a spectroscopic point of view, since it results from global fits and that the comparison with the ATMOS spectra shows either analogous simulations or better ones (in band D), it is possible to conclude that the CSCD is likely to give better results than HITRAN-2K.

Eventually the CO_2 line parameters included in the new version of the MIPAS database are:

– for the four most abundant isotopic variants of CO_2, namely $^{12}C^{16}O_2$, $^{13}C^{16}O_2$, $^{16}O^{12}C^{18}O$, and $^{16}O^{12}C^{17}O$, the line parameters of CDSD;

– for the other isotopic variants of CO_2 the line parameters of HITRAN-96.

3. Ozone O_3

3.1. Ozone $^{16}O_3$

The ozone molecule $^{16}O_3$ has been recently the subject of extensive laboratory studies performed by four different groups[28–31] in the 10 μm region in order to improve line positions and intensities in this spectral domain which is extensively used for atmospheric retrievals by several instruments and in particular by MIPAS. The four sets of experimental data have been compared leading to the following conclusion (see Ref. 32 for more details):

The three sets of data from Refs. 29–31 agree very well as far as absolute intensities are concerned (variance of ≅ 0.8%, 1σ standard deviation of ≅ 1.7%) whereas intensities from Ref. 28 are consistently ≅ 4% higher.

As a consequence it was decided to rely on the sets of consistent intensities from Refs. 29–31 and these intensities were fitted to derive the relevant transition moment constants.[32] Using these constants a new line list was generated for the two bands absorbing at 10 μm, namely, ν_1 (HIT4–1) and ν_3 (HIT5–1).

When comparing to the HITRAN data which are those from Ref. 33, one obtains the following intensity ratios:

band	ν_1	ν_3
HIT96 / NEWCAL	1.044(35)	1.035(14)

Also the new line list was validated against the ATMOS data and the results are gathered in Table 6.

Table 6. Comparisons of simulated and observed ATMOS spectra using HITRAN-96 and the new ozone data

Altitude, km	34	26
Spectral domain, cm^{-1}	1023–1170	1065–1170
RMS (CAL / HIT96)	0.669 / 0.725	0.460 / 0.482
Number of intervals where CAL gives better results	44 of 49	33 of 35

It appears that:

– the overall RMS is, for the two altitudes, better with the new data than with the HITRAN-96 data;

– the statistical analysis of the residuals obtained for the 3 cm^{-1} wide intervals covering the spectral domains usable from the ATMOS spectra shows that for more than 90% of the intervals the new data give better results.

This proves that, on a relative basis, the new data allow one to perform better simulations.

As a consequence, it was decided to include the new data in the MIPAS database. More precisely:

– the cold bands ν_1 (HIT4–1), ν_3 (HIT5–1), and ν_2 (HIT2–1) (the latter being an additional measurement provided by Ref. 31) have been included in the MIPAS database;

– the intensities of all the other bands (hot bands, isotopic species) were divided by 1.04 to account for the change in the absolute intensities of the cold bands.

3.2. Less abundant ozone isotopic variants

To complete the HITRAN database the 10 μm bands (ν_1 and ν_3) of $^{16}O^{16}O^{17}O$ and $^{16}O^{17}O^{16}O$ have been added to the MIPAS database. Using the results in Ref. 35 and 36 these bands have indeed been observed in the atmosphere.[34] Furthermore the strongest ozone bands $\nu_1 + \nu_3$ in the 4.8 μm region for $^{16}O^{16}O^{18}O$, $^{16}O^{18}O^{16}O$, $^{16}O^{16}O^{17}O$, and $^{16}O^{17}O^{16}O$ have been observed in atmospheric spectra[37,38] and accordingly the line parameters of these bands have been included into the database. Concerning this spectral region it is worth stressing the following points:

– There are 3 interacting bands, namely, $\nu_1 + \nu_3$, $2\nu_1$, and $2\nu_3$, absorbing in the region around 4.8 μm. As a consequence the spectroscopic analyses[39,40] were performed taking into account the vibro-rotational resonances affecting the energy levels and the line intensities. However the main problem is that only $\nu_1 + \nu_3$ (it is a strong band) was observed in the laboratory spectra whereas the two other bands were not. Accordingly the Hamiltonian constants of these two latter bands are extrapolated constants preventing one to calculate precisely the corresponding line positions.

– Also, whereas the relative line intensities of the strong $\nu_1 + \nu_3$ bands are likely to be more or less correct, this is probably not the case for the weak $2\nu_1$ and $2\nu_3$ bands because they are very sensitive to the vibration-rotation interactions.

Finally one has to recognize that it is extremely difficult to estimate the uncertainty on the absolute intensities at 4.8 μm. Indeed the line intensities of the isotopic species were calculated using the transition moment of the main isotope. Clearly this is theoretically incorrect but, unfortunately, the theory does not allow transferring properly the transitions moments from $^{16}O_3$ to the other isotopic species (second derivatives with respect to the normal coordinates of the transition moment operator are involved). In fact, at this stage, we estimate that the absolute intensities

of the $\nu_1 + \nu_3$ bands of $^{16}O^{18}O^{16}O$, $^{16}O^{16}O^{18}O$, $^{16}O^{17}O^{16}O$, and $^{16}O^{16}O^{17}O$ are not known to better than 30-40% (conservative estimation).

As a conclusion, given the above considerations, we have introduced in the MIPAS database only the line parameters of the strong $\nu_1 + \nu_3$ bands keeping in mind that their absolute intensities cannot be assumed at this stage to be better known than 30–40%. Consequently we advise the reader that the corresponding lines cannot be used to derive precisely the amount of $^{16}O^{18}O^{16}O$, $^{16}O^{16}O^{18}O$, $^{16}O^{17}O^{16}O$, and $^{16}O^{16}O^{17}O$ in the atmosphere. However they are useful as "interfering" lines.

4. Methane $^{12}CH_4$, $^{13}CH_4$, CH_3D

The file 06.HIT01.par, which is not included in HITRAN-2K, is a total replacement of the 1996 spectroscopic parameters in the MIPAS channels. In this new database, predictions from recent successful modeling of positions and intensities for all three isotopes[41,42,43] were merged. The accuracy ranged from 0.0001 to 0.005 cm^{-1} for the positions and from 3 to 15% for intensities, with stronger transitions of the fundamentals in each isotope having better quality. Line shape coefficients for the Voigt profile were assessed using the most recent measurements of broadening coefficients (see Refs. 44, 45, and 46 and the references therein). Measured air-broadened line widths accurate to 3% were inserted for several hundred of the methane transitions, and default values for the remainder were determined with 20% accuracy by averaging measured values according to *m* (where *m* is the lower state *J* for *P* and *Q*-branch lines and the upper state *J* for the *R* branch). Nevertheless, accurate CH_4 line widths and pressure shifts are generally unavailable for the intermediate strength lines that contribute to the MIPAS signal. Better broadening information was available for CH_3D because air- and self-broadened coefficients of many more transitions had been measured, and widths of unmeasured transitions could be approximated to 6% by an empirical expression (see Ref. 47 and the references therein). The total list (available in 2001 on the HITRAN website in the update section) is described in a more detail by Brown et al. (Ref. 48). Many lines weaker than $1 \cdot 10^{-24}$ $cm^{-1}/(molecule \cdot cm^{-2})$ were included for the benefit of planetary and stellar applications. Finally, it is worth stressing that recently the IMK group[49] reported that in the 1202 cm^{-1} spectral region the fit quality of ground based FTIR atmospheric spectra was decreasing in terms of spectral residuals when using the updated spectral parameters. A careful analysis by the IMK group[49] showed that, for some lines, there were problems with some new pressure shifts and to a lesser extent with some new pressure broadening coefficients. It turned out that some of the parameters were inadvertently changed and a new line list was provided.[50] This new data set was compared with the previous one (HITRAN-96) using ATMOS spectra. The statistical analysis of the residuals in the main absorption ranges of CH_4 (1050–1899 cm^{-1} and 2149–2500 cm^{-1}) using ATMOS spectra recorded at altitude of 23.334 km (see Table 7) confirms that the new data are more reliable. Accordingly, in the MIPAS database the methane HITRAN-96 data have been replaced by the new data.

Table 7. Comparisons of simulated and observed ATMOS spectra using HITRAN-96 and the new methane data at 23.3 km

Band	Spectral domain, cm^{-1}	Number of intervals where new data give better results
AB	1065–1170	34 of 35
B	1215–1278; 1350–1500	45 of 71
C	1570–1690	27 of 36
D	2123–2258	30 of 46

5. Nitrogen dioxide $^{14}NO_2$

The 6.2 μm region is widely used to retrieve atmospheric NO_2 profiles from balloon borne or satellite instruments since it corresponds by far to the strongest absorption of this molecule: the ν_3 band (HIT 5–1).

As far as spectroscopy is concerned, due to the spin-rotation interaction the infrared vibration-rotation lines appear as doublets. This spin-rotation interaction can be treated either through a perturbation method or directly, the latter method giving much more accurate results.

In HITRAN-96 only two bands appear in the 6.2 μm region:

- The fundamental ν_3 (HIT 5–1) band for which the spin-rotation interaction is taken fully into account.[51]
- The first hot band $\nu_2 + \nu_3 - \nu_2$ (HIT 8–2) for which this interaction is treated through a perturbation method,[52] hence providing one with the results of a quality not sufficient for an experiment like MIPAS.

It is worth noticing that no other hot band is available in this spectral region in the HITRAN database preventing one from dealing with possible NLTE phenomena.

Based on recent spectroscopic studies, new spectral parameters were generated and included in the MIPAS database.

They are:

- the band system[53] {011,030} ← (010) which replaces the first hot band $\nu_2 + \nu_3 - \nu_2$,
- the band system[54] {120,101} ← {100, 020, 001}, the strongest band of which is $\nu_1 + \nu_3 - \nu_1$ (HIT 13–4),
- the band system[55] {040, 021, 002} ← {100, 020, 001} the strongest bands of which are $2\nu_3 - \nu_3$ (HIT 14–5) and $2\nu_2 + \nu_3 - 2\nu_2$ (HIT 11–3),
- the band system[56] {022, 003} ← {040, 021, 002} the strongest bands of which are $3\nu_3 - 2\nu_3$ (HIT 27–14) and $2\nu_2 + 2\nu_3 - (2\nu_2 + \nu_3)$ (HIT 23–11).

Table 8 presents the characteristics of the new 23 bands, which have been included in the MIPAS database.

Table 8. Summary of the NO_2 hot bands included in the MIPAS database

#	Band	XMIN	XMAX	SMIN	SMAX	STOT	NB
1	1 0 1 0 0 1	1142.0215	1612.7745	0.180D–27	0.113D–24	0.381D–22	5268
2	1 2 0 0 2 0	1144.4766	1517.8400	0.180D–27	0.337D–25	0.157D–22	4425
3	1 0 1 0 2 0	1175.6815	1612.1739	0.183D–27	0.270D–26	0.199D–24	253
4	0 2 2 0 2 1	1226.0473	1881.4318	0.176D–31	0.757D–25	0.307D–22	11892
5	1 2 0 0 0 1	1327.0051	1365.8081	0.181D–27	0.469D–27	0.176D–26	7
6	0 0 3 0 0 2	1348.1076	1788.3529	0.176D–31	0.664D–25	0.297D–22	9679
7	0 2 2 0 0 2	1353.0833	1803.4869	0.176D–31	0.252D–26	0.756D–25	3554
8	0 4 0 0 2 0	1367.6299	1727.4077	0.388D–28	0.198D–22	0.142D–20	4772
9	0 3 0 0 1 0	1372.8892	1797.4293	0.261D–26	0.659D–22	0.121D–20	5783
10	0 2 2 0 4 0	1380.6887	1752.2183	0.176D–31	0.175D–25	0.123D–23	6561
11	0 2 1 0 2 0	1390.7158	1833.4969	0.389D–28	0.882D–22	0.352D–19	7571
12	0 2 1 0 0 1	1395.0056	1726.4321	0.388D–28	0.460D–23	0.427D–21	2554
13	1 2 0 1 0 0	1397.1888	1695.0039	0.180D–27	0.208D–24	0.311D–22	2591
14	0 0 2 0 0 1	1401.6565	1843.2518	0.388D–28	0.988D–22	0.433D–19	7687
15	0 1 1 0 1 0	1410.5613	1836.3982	0.261D–26	0.338D–20	0.145D–17	9215
16	0 4 0 0 0 1	1430.0087	1678.6526	0.391D–28	0.319D–26	0.161D–24	504
17	0 0 3 0 2 1	1432.8641	1739.7821	0.176D–31	0.263D–26	0.138D–24	2267
18	1 0 1 1 0 0	1457.7296	1828.6348	0.180D–27	0.209D–21	0.912D–19	7454
19	0 0 3 0 4 0	1459.2100	1731.3784	0.176D–31	0.199D–29	0.105D–27	616
20	0 0 2 0 2 0	1507.8867	1768.1095	0.388D–28	0.326D–23	0.299D–21	1008
21	0 0 2 1 0 0	1526.4612	2035.5122	0.388D–28	0.719D–24	0.289D–21	8727
22	0 2 1 1 0 0	1532.0191	1984.5359	0.388D–28	0.105D–25	0.193D–23	1458
23	0 4 0 1 0 0	1808.9781	1855.6778	0.388D–28	0.392D–28	0.780D–28	2

The meaning of the different columns is the same as in Table 4.

As far as the air-broadening coefficients γ_{air} are concerned, recently a number of studies have dealt with the line widths of the NO_2 molecule. In particular Ref. 57 provides an overview and a comparison of various papers in order to derive the air-broadening coefficients and their *n*-temperature dependence for the NO_2 absorption features in the 13200–42000 cm^{-1} range.

Comparing a number of experimental results (see Ref. 57 for details) they recommend the values:

γ_{air} (296 K) = 0.080(3) $cm^{\$1}$ / atm, n = 0.8(2).

These values are to be compared:

– to the values given in HITRAN-96 or HITRAN-2K:

γ_{air} (296 K) = 0.067 $cm^{\$1}$ / atm, n = 0.5;

– or to the values given in HITRAN-01:

γ_{air} (296 K) ≈ 0.0707** $cm^{\$1}$ / atm, n = 0.97***;

– or to the values derived from UV spectra (Ref. 62):

γ_{air} (296 K) = 0.134(10) $cm^{\$1}$ / atm, n = 1.03(80).

Note that the authors recognize in their paper that the value obtained for γ_{air} is questionable because of the line-mixing and resolution problems.

Given these results and the errors associated and, until new experimental or theoretical results are available, we are using in the MIPAS database:

γ_{air} (296 K) = (0.074 / 0.71) γ_{air} (HITRAN-01), n = 0.97.

** Mean value calculated from all individual values of Dana et al. (Ref. 58).

*** Value derived from Refs. 59–61.

Also instead of no value HITRAN-01 gives the value of 0.095 cm^{-1} / atm for the self-broadening coefficient. This value seems reasonable and we have introduced it in the MIPAS database.

6. Nitric acid HNO_3

The 11 μm bands of nitric acid are widely used by infrared remote sensing techniques since they are centered in an atmospheric window and therefore present the advantage of being relatively free from interfering lines from other species. The 11 μm spectral region involves mainly two interacting cold bands ν_5 and $2\nu_9$ and two hot bands $\nu_5 + \nu_9 - \nu_9$ and $3\nu_9 - \nu_9$ located at 885.424 and 830.6 cm^{-1}, respectively.

6.1. The hot band $\nu_5 + \nu_9 - \nu_9$

We summarize here only the important points since a detailed analysis can be found in Ref. 63. Performing simulations of ATMOS spectra using HITRAN-96 or HITRAN-2K it was shown that, even if better results are obtained with HITRAN-2K, the agreement was far from being satisfactory (shift and shape of the absorption peak not correct) when modeling the hot band absorption. It was then decided to perform a spectroscopic study of the hot band[63] and the results of a modeling of an ATMOS spectrum using the new data are presented in Fig. 1. The excellent agreement between observation and calculation is obvious. Accordingly, the new data were included in the MIPAS database.

The $3\nu_9 - \nu_9$ band (HIT 23–19) was also calculated and included in the MIPAS database: it is worth noticing that the spectral parameters for this band present in HITRAN-96 are not correct (it is no longer

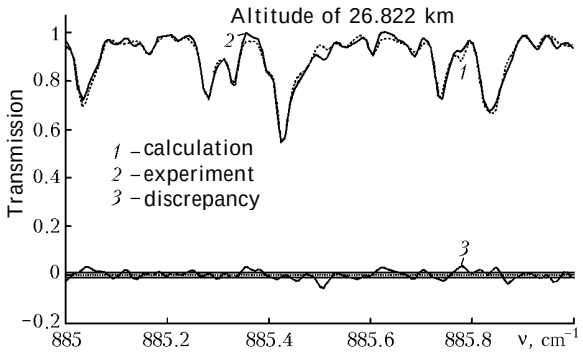

Fig. 1. Simulation of an ATMOS spectrum around 885 cm^{-1} using the new parameters for the $\nu_5 + \nu_9 - \nu_9$ hot band.

included in HITRAN-2K). However the effect of these new data on atmospheric simulations could not yet be checked properly because the ATMOS data at our disposal were not of sufficient quality in the corresponding spectral domain.

6.2. Absolute intensities

Recently a paper dealing with HNO_3 absolute line intensities in the 11 μm spectral region was published[64] providing one with a total band intensity of 560 (5%) cm^{-2}/atm, for the two cold bands ν_5 and $2\nu_9$. This value which corresponds to the average of previous low resolution studies (see Refs. 65–68) is different from the value of 637 cm^{-2}/atm, used in the HITRAN database.[58] Given the extensive number of transitions reported, we have decided to use this new value for the total band intensities of the cold bands at 11 μm. Accordingly the individual line intensities of the bands ν_5 (HIT 18–14), $2\nu_9$ (HIT 21–14), ν_3 (HIT 27–14), and ν_4 (HIT 17–14) have been multiplied by the factor 0.879. However, it should be noted that the reported absolute accuracy for the intensity is 5%, and this result awaits independent verification. The consistency of the cold bands and the hot band line parameters was eventually checked using preliminary MIPAS data.

7. Hypochlorous acid HOCl

Recent studies[69,70] of the spectroscopic properties of HOCl have shown that the HITRAN-96 spectral parameters concerning the ^{35}Cl and ^{37}Cl isotopic variants of this species were not of sufficient quality both for the line positions and intensities. As far as the MIPAS database is concerned, the main problem was related to the line intensities in the 8.1 μm spectral region. Indeed, this molecule is unstable and always exists in the equilibrium

$$H_2O + Cl_2O \leftrightarrows 2\ HOCl.$$

The main difficulty when measuring line intensities is then to estimate its partial pressure in the cell. Different methods can be used (see Ref. 70 for their description), but when one looks at the literature it appears that there is a huge scatter among the various results concerning the total band intensities (Table 8 of Ref. 70). To avoid this difficulty, the method used in Ref. 70 was to measure simultaneously the far infrared and the 8.1 μm line intensities. Since the intensities can be precisely calculated in the far infrared using the dipole moment derived from Stark experiments, one can use them to estimate accurately the partial pressure of HOCl and hence to get reliable intensities at 8.1 μm. These new intensities are on the average 66% lower than the HITRAN-96 ones. Such a change is huge but it is worth stressing that the newly measured line intensities have been fully confirmed by very recent *ab initio* studies.[71] The new data have been included in the MIPAS database.

8. Carbonyl fluoride COF_2

Initially an update of the line parameters of COF_2 was undertaken[72] because the rotational assignments of the transitions were incorrect in HITRAN. The COF_2 line parameters in the 5.2 μm spectral region correspond to 3 bands ν_1 (HIT 5–1), $2\nu_2$ (HIT 12–1), and $2\nu_3 + \nu_6$ (HIT 14–1), which are in strong interaction.[72] Among them, the strongest band is the ν_1 fundamental band, the two others borrowing their intensities from this band. Indeed since ν_1 is a fundamental band and since $2\nu_2$ and $2\nu_3 + \nu_6$ are overtone and combination bands, it is likely that these two latter bands have a much smaller intensity than the fundamental one. Accordingly the relative intensities were partitioned between the three bands assuming a non-zero dipole moment for the ν_1 band and letting the Fermi and Coriolis interactions transfer intensity into the two weaker bands. The total band intensity of the three bands system was scaled using a vibrational partition function of ~ 1.15 to the best three reported low resolution integrated absorption (Refs. 73–75) and a line list was generated.[72] These data have been compared to the data included in HITRAN-2K and the following comments can be made:

– The new data have slightly stronger intensities than the HITRAN-2K ones. The mean ratio HIT/CAL is about 0.973 for the lines in common. This is not fully consistent with the ratio of 0.930 obtained when comparing the total intensities of the band systems: $0.568 \cdot 10^{-16}$ for the new data versus $0.528 \cdot 10^{-16}$ for the HITRAN-2K data but can be explained by the fact that the new data have a smaller intensity cut off. Therefore a lot of weak lines exist which add up to increase the total band intensities.

– The weak $2\nu_3 + \nu_6$ band is not included in HITRAN-2K.

As a conclusion the new data were introduced in the MIPAS database since they are more complete and since the rotational assignments of the transitions are correct. Also, thanks to the better theoretical analysis, the new individual line intensities are likely to be better than the HITRAN-2K ones.

Conclusion

This paper describes the MIPAS database as of January 2003. The efforts were mainly devoted to the improvement of the line parameters of the CO_2 molecule (pressure and temperature profiles) and of the target species (O_3, H_2O, CH_4, HNO_3, N_2O, NO_2). The paper discusses mainly the previously unpublished line parameters and how they were assessed. Finally, even if we are aware that no compilation is perfect, we hope that the new database represents an improvement for the analysis and retrieval of MIPAS spectra.

Acknowledgments

The authors are indebted to all the persons who provided evaluations and comments. In particular we wish to thank N. Glatthor, G. Stiller, F. Hase, T. von Clarmann, H. Oelhaf, J. Vander Auwera, M. Birk, G. Wagner, M.A.H. Smith, J. Orphal, Vl. Perevalov, S.A. Tashkun, A. Barbe, H. Nett, J. Langen, W.J. Lafferty, R.A. Toth, and L.S. Rothman.

We thank also gratefully F.W. Irion, G.C. Toon, and M.R. Gunson for making available to us the ATMOS spectra.

Support from ESA (Contract No: 11717/95/NL/CN) and from the European Community through the project AMIL2DA (Project EVG1–CT–1999–00015) is gratefully acknowledged.

References

1. M. Ridolfi, B. Carli, M. Carlotti, T.V. Clarmann, B.M. Dinelli, A. Dudhia, J.-M. Flaud, M. Hoepfner, P.E. Morris, P. Raspollini, G. Stiller, and R.J. Wells, *Optimized forward model and retrieval scheme for MIPAS near-real-time data processing*, Appl. Opt. **39**, No. 8, 1323$ 1340 (2000).

2. A. Dudhia, V.L. Jay and C.D. Rodgers, *Microwindow selection for high-spectral-resolution sounders*, Appl. Opt. **41**, 3665–3673 (2002).

3. M. Lopez-Puertas and F.W. Taylor, *Non-LTE Radiative Transfer in the Atmosphere* (World Scientific, 2002).

4. L.S. Rothman, C.P. Rinsland, A. Goldman, S.T. Massie, D.P. Edwards, J.-M. Flaud, A. Perrin, C. Camy-Peyret, V. Dana, J.-Y. Mandin, J. Schroeder, A.Mc. Cann, R.R. Gamache, R.B. Wattson, K. Yoshino, K.V. Chance, K.W. Jucks, L.R. Brown, V. Nemtchinov, and P. Varanasi, *The HITRAN molecular spectroscopic data base and HAWKS (HITRAN Atmospheric Work Station): 1996 edition*, J. Quant. Spectrosc. Radiat. Transfer **60**, 665–710 (1998).

5. N. Jacquinet-Husson, E. Arie, J. Ballard, A. Barbe, G. Bjoraker, B. Bonnet, L.R. Brown, C. Camy-Peyret, J.P. Champion, A. Chedin, A. Chursin, C. Clerbaux, G. Duxbury, J.-M. Flaud, N. Fourrie, A. Fayt, G. Graner, R. Gamache, A. Goldman, Vl. Golovko, G. Guelachvili, J.-M. Hertmann, J.C. Hilico, J. Hillman, G. Lefevre, E. Lellouch, S.N. Mikhailenko, O.V. Naumenko, V. Nemtchinov, D.A. Newnham, A. Nikitin, J. Orphal, A. Perrin, D.C. Reuter, C.P. Rinsland, L. Rosenmann, L.S. Rothman, N.A. Scott, J. Selby, L.N. Sinitsa, J.M. Sirota, A.M. Smith, K.M. Smith, Vl.G. Tyuterev, R.H. Tipping, S. Urban, P. Varanasi, and M. Weber, *The 1997 spectroscopic GEISA databank*, J. Quant. Spectrosc. Radiat. Transfer **62**, 205–254 (1999).

6. M.R. Gunson et al., *The Atmospheric Trace Molecule Spectroscopy (ATMOS) experiment: Deployment on the ATLAS Space Shuttle missions*, Geophys. Res. Lett. **23**, No. 17, 2333–2336 (1996).

7. ftp://cfa-ftp.harvard.edu

8. L.H. Coudert, *Analysis of the rotational energy levels of water and determination of the potential energy function for the bending* ν_2 *mode*, J. Mol. Spectrosc. **165,** 406 (1994).

9. R. Lanquetin, L.H. Coudert, and C. Camy-Peyret, *High-lying rotational levels of water: an analysis of the energy levels of the five first vibrational states*, J. Mol. Spectrosc. **206,** 83 (2001).

10. L.H. Coudert, *Line frequency and line intensity analyses of water vapor*, Molec. Phys. **96,** 941 (1999).

11. J.W.C. Johns, *High-resolution far-infrared spectra of several isotopic species of* H_2O, J. Opt. Soc. Am. B **2,** 1340 (1985).

12. Paso and Horneman, *High-resolution rotational absorption spectra of* $H_2{}^{16}O$, $HD^{16}O$, *and* $D_2{}^{16}O$ *between* 110 *and* 500 cm^{-1}, J. Opt. Soc. Am. B **12,** 1813 (1995).

13. R.A. Toth, *Water vapor measurements between* 590 *and* 2582 cm^{-1}: *Line positions and strengths*, J. Mol. Spectrosc. **190,** 379 (1998).

14. R.A. Toth, $\nu_1 - \nu_2$, $\nu_3 - \nu_2$, ν_1, *and* ν_3 *bands of* $H_2{}^{16}O$: *line positions and strengths*, J. Opt. Soc. Am B **10,** 2006 (1993).

15. R.A. Toth, $\nu_2 - \nu_2$ *and* $2\nu_2$ *bands of* $H_2{}^{16}O$, $H_2{}^{17}O$ *and* $H_2{}^{18}O$: *line positions and strengths*, J. Opt. Soc. Am B **10,** 1526 (1993).

16. C.P. Rinsland, A. Goldman, M.A.H. Smith, and V.M. Devi, *Measurements of Lorentz air-broadening coefficients and relative intensities in the* $H_2{}^{16}O$ *pure rotational and* ν_2 *bands from long horizontal path atmospheric spectra*, Appl. Opt. **30,** 1427 (1991).

17. L.R. Brown and Plymate, H_2*-broadened* $H_2{}^{16}O$ *in four infrared bands between* 55 *and* 4045 cm^{-1}, J. Quant. Spectrosc. Radiat. Transfer **56,** 263 (1996).

18. R.A. Toth, Private communication (2001).

19. R.B. Wattson and L.S. Rothman, *Direct numerical diagonalization: wave of the future*, J. Quant. Spectrosc. Radiat. Transfer **48**, 763–780 (1992).

20. S.A. Tashkun, V.I. Perevalov, J.L. Teffo, L.S. Rothman, and Vl.G. Tyuterev, *Global fitting of* CO_2 *vibration-rotation line positions using the effective Hamiltonian approach*, J. Quant. Spectrosc. Radiat. Transfer **60**, 785–801 (1998).

21. S.A. Tashkun, V.I. Perevalov, J.-L. Teffo, and Vl.G. Tyuterev, *Global fitting of* $^{12}C^{16}O_2$ *vibration-rotation line intensities using the effective operator approach*, J. Quant. Spectrosc. Radiat. Transfer **62**, 571–598 (1999).

22. S.A. Tashkun, V.I. Perevalov, and J.-L. Teffo, *CDSD: a high precision high temperature spectroscopic databank of the* CO_2 *molecule*, in: V^e *Colloque Atmospheric Spectroscopy Applications* (Reims, 1999).

23. S.A. Tashkun, V.I. Perevalov, J.-L. Teffo, M. Lecoutre, T.R. Huet, A. Campargue, D. Bailly, and M.P. Esplin, $^{13}C^{16}O_2$: *Global treatment of vibrational-rotational spectra and first observations of the* $2\nu_1 + 5\nu_3$ *and* $\nu_1 + 2\nu_2 + 5\nu_3$ *absorption bands*, J. Mol. Spectrosc. **200**, 162–176 (2000).

24. J.-L. Teffo, C. Claveau, Q. Kou, G. Guelachvili, A. Ubelmann, V.I. Perevalov and S.A. Tashkun, *Line intensities of* $^{12}C^{16}O_2$ *in the* 1.2–1.4 μm *spectral region*, J. Mol. Spectrosc. **201**, 249–255 (2000).

25. S.A. Tashkun, V.I. Perevalov and J.-L. Teffo, *Global fittings of the vibrational-rotational line positions of the* $^{16}O^{12}C^{17}O$ *and* $^{16}O^{12}C^{18}O$ *isotopic species of carbon dioxide*, J. Mol. Spectrosc. **210**, 137–145 (2001).

26. J.-L. Teffo, L. Daumont, C. Claveau, A. Valentin, V.I. Perevalov and S.A. Tashkun, *Infrared spectra of the* $^{16}O^{12}C^{17}O$ *and* $^{16}O^{12}C^{18}O$ *species of carbon dioxide: The region* 500–1500 cm^{-1}, J. Mol. Spectrosc. **213**, 145–152 (2002).
27. J.-L. Teffo, L. Daumont, C. Claveau, A. Valentin, V.I. Perevalov and S.A. Tashkun, *Infrared spectra of the* $^{16}O^{12}C^{17}O$ *and* $^{16}O^{12}C^{18}O$ *species of carbon dioxide: The region* 1500–3000 cm^{-1}, J. Mol. Spectrosc. (submitted).
28. M.A.H. Smith, V. Malathy Devi, D.C. Benner and C.P. Rinsland, *Absolute intensities of* $^{16}O_3$ *lines in the* 9–11 μm *region*, J. Geophys. Res. **106**, 9909–9921 (2001).
29. C. Claveau, C. Camy-Peyret, A. Valentin and J.-M. Flaud, *Absolute intensities of the* ν_1 *and* ν_3 *bands of* $^{16}O_3$, J. Mol. Spectrosc. **206**, 115–125 (2001).
30. M.R. De Backer-Barilly and A. Barbe, *Absolute intensities of the* 10 μm *bands of* $^{16}O_3$, J. Mol. Spectrosc. **205**, 43–53 (2001).
31. G. Wagner, M. Birk, F. Schreir, and J.-M. Flaud, *Spectroscopic database of ozone in the fundamental spectral region*, J. Geophys. Res. (in press, 2002).
32. J.M. Flaud, G. Wagner, M. Birk, C. Camy-Peyret, C. Claveau, M.R. De Backer-Barilly, A. Barbe, and C. Piccolo, *The ozone absorption around* 10 μm, J. Geophys. Res. (in press, 2003).
33. J.-M. Flaud, C. Camy-Peyret, C.P. Rinsland, M.A.H. Smith and V. Malathy Devi, *Atlas of Ozone Spectral Parameters from Microwave to Medium Infrared* (Academic Press, Cambridge, Massachusetts, 1990).
34. C.P. Rinsland, J.-M. Flaud, A. Goldman, A. Perrin, C. Camy-Peyret, M.A.H. Smith, V. Malathy Devi, D.C. Benner, A. Barbe, T.M. Stephen, and F.J. Murcray, *Spectroscopic parameters for ozone and its isotopes: current status, prospects for improvement and the identification of* $^{16}O^{16}O^{17}O$ *and* $^{16}O^{17}O^{16}O$ *lines in infrared ground based and stratospheric solar absorption spectra*, J. Quant. Spectrosc. Radiat. Transfer **60**, 803–814 (1998).
35. M. Heyart, A. Perrin, J-M. Flaud, C. Camy-Peyret, C.P. Rinsland, M.A.H. Smith, and V. Malathy Devi, *The* ν_1 *and* ν_3 *bands of* $^{6}O^{17}O^{16}O$. *Line positions and intensities*, J. Mol. Spectrosc. **156**, 210–216 (1992).
36. M. Heyart, A. Perrin, J-M. Flaud, C. Camy-Peyret, C.P. Rinsland, M.A.H. Smith, and V. Malathy Devi, *The hybrid type* ν_1 *and* ν_3 *bands of* $^{16}O^{16}O^{17}O$: *line positions and intensities*, J. Mol. Spectrosc. **157**, 524–531 (1993).
37. D.W. Arlander, A. Barbe, M.T. Bourgeois, A. Hamdouni, J.-M. Flaud, C. Camy-Peyret, and Ph. Demoulin, *The identification of* $^{16}O^{18}O^{16}O$ *and* $^{16}O^{16}O^{18}O$ *isotopes in high resolution ground-based spectra*, J. Quant. Spectrosc. Radiat. Transfer **52**, 267–272 (1994).
38. A. Goldman, C.P. Rinsland, A. Perrin, J.-M. Flaud, A. Barbe, C. Camy-Peyret, M.T. Coffey, W.G. Mankin, J.W. Hanningan, T.M. Stephen, V. Malathy Devi, and M.A.H. Smith, *Weak ozone isotopic absorption in the* 5 μm *region from FTIR solar spectra*, J. Quant. Spectrosc. Radiat. Transfer **74**, 133–138 (2002).
39. J.-M. Flaud, M.T. Bourgeois, A. Barbe, J.-J. Plateaux, and C. Camy-Peyret, *The* $\nu_1 + \nu_3$ *bands of* $^{16}O^{18}O^{16}O$ *and* $^{16}O^{16}O^{18}O$, J. Mol. Spectrosc. **165**, 464–469 (1994).
40. A. Perrin, J.-M. Flaud, F. Keller, M.A.H. Smith, C.P. Rinsland, V. Malathy Devi, D.C. Benner, T.M. Stephen, and A. Goldman, *The* $\nu_1 + \nu_3$ *bands of* $^{16}O^{17}O^{16}O$ *and* $^{16}O^{16}O^{17}O$ *isotopomers of ozone*, J. Mol. Spectrosc. **207**, 54–59 (2001).
41. J.P. Champion, J.C. Hilico, C. Wenger, and L.R. Brown, *Analysis of the* ν_2/ν_4 *dyad of* $^{12}CH_4$ *and* $^{13}CH_4$, J. Mol. Spectrosc. **133**, 256–272 (1989).
42. O. Ouardi, J.C. Hilico, M. Loete, and L.R. Brown, *The hot bands of methane between* 5 *and* 10 μm, J. Mol. Spectrosc. **180**, 311–322 (1996.)
43. A. Nikitin, L.R. Brown, L. Fejard, J.P. Champion, and VI.G. Tyuterev, *Analysis of the* CH_3D *nonad from* 2000–3300 cm^{-1}, J. Mol. Spectrosc. (in press).
44. D.C. Benner, V.M. Devi, M.A.H. Smith, and C.P. Rinsland, *Air-broadening,* N_2*-broadening, and* O_2*-broadening and shift coefficients in the* ν_3 *spectral region of* $^{12}CH_4$, J. Quant. Spectrosc. Radiat. Transfer **50**, 65–89 (1993).
45. M.A.H. Smith, C.P. Rinsland, V.M. Devi, and D.C. Benner, *Temperature-dependence of broadening and shifts of methane lines in the* ν_4 *band*, Spectrochim. Acta **48A**, 1257–1272 (1992).
46. V.M. Devi, D.C. Benner, M.A.H. Smith, and C.P. Rinsland, *Temperature-dependence of Lorentz air-broadening and pressure-shift coefficients of* $^{12}CH_4$ *lines in the* 2.3-μm *spectral region*, J. Quant. Spectrosc. Radiat. Transfer **51**, 439–465 (1994).
47. V.M. Devi, D.C. Benner, M.A.H. Smith, C.P. Rinsland, and L.R. Brown, *Self- and* N_2*-broadening, pressure induced shift and line mixing in the* ν_5 *band of* $^{12}CH_3D$ *using a multi-spectrum fitting technique*, J. Quant. Spectrosc. Radiat. Transfer **74**, 1–41 (2002).
48. L. Brown et al., *Methane line parameters in HITRAN* (in prep. for J. Quant. Spectrosc. Radiat. Transfer).
49. F. Hase, N. Glatthor, and G. Stiller, Private communication (2002).
50. L.R. Brown, Private communication (2002).
51. A. Perrin, J.-M. Flaud, C. Camy-Peyret, A.M. Vasserot, G. Guelachvili, A. Goldman, F.J. Murcray, and R.D. Blatherwick, *The* ν_1, $2\nu_2$ *and* ν_3 *interacting bands of* NO_2: *line positions and intensities*, J. Mol. Spectrosc. **154**, 391–406 (1992).
52. C. Camy-Peyret, J.-M. Flaud and A. Perrin, *Improved line parameters for the* ν_3 *and* $\nu_2 + \nu_3 - \nu_2$ *bands of* NO_2, J. Mol. Spectrosc. **95**, 72–79 (1982).
53. A. Perrin, J.-M. Flaud, C. Camy-Peyret, D. Hurtmans, M. Herman and G. Guelachvili, *The* $\nu_2 + \nu_3$ *and* $\nu_2 + \nu_3 - \nu_2$ *bands of* NO_2: *line positions and intensities*, J. Mol. Spectrosc. **168**, 54–66 (1994).
54. J.Y. Mandin, V. Dana, A. Perrin, J.-M. Flaud, C. Camy-Peyret, L. Régalia and A. Barbe, *The* $\{\nu_1 + 2\nu_2, \nu_1 + \nu_3\}$ *bands of* NO_2: *line positions and intensities, line intensities in the* $\nu_1 + \nu_2 + \nu_3 - \nu_2$ *hot band*, J. Mol. Spectrosc. **181**, 379–388 (1997).
55. A. Perrin, J.-M. Flaud, C. Camy-Peyret, D. Hurtmans and M. Herman, *The* $\{2\nu_3, 4\nu_2, 2\nu_2 + \nu_3\}$ *and* $2\nu_3 - \nu_3$ *bands of* NO_2: *line positions and intensities*, J. Mol. Spectrosc. **177**, 58–65 (1996).
56. T.M. Stephen, A. Goldman, A. Perrin, J.-M. Flaud, F. Keller and C.P. Rinsland, *New high resolution analysis of the* $3\nu_3$ *and* $2\nu_1 + \nu_3$ *bands of* NO_2 *by Fourier transform spectroscopy*, J. Mol. Spectrosc. **201**, 134–142 (2000).
57. A.C. Vandaele, C. Hermans, S. Fally, M. Carleer, M.-F. Merienne, A. Jenouvrier and R. Colin, *Absorption cross section of* NO_2: *Simulation of temperature and pressure effects*, J. Quant. Spectrosc. Radiat. Transfer (in press).
58. V. Dana, J.-Y. Mandin, M.-Y. Allout, A. Perrin, L. Regalia, A. Barbe, and X. Thomas, *Broadening parameters of* NO_2 *lines in the* 3.4 μm *spectral region*, J. Quant. Spectrosc. Radiat. Transfer **57**, 445–457 (1997).
59. V. Malathy Devi, B. Fridovich, G.D. Jones, D.G.S. Snyder, P.P. Das, J.-M. Flaud, C. Camy-Peyret, and K. Narahari Rao, *Tunable diode laser spectroscopy of* NO_2 *at* 6.2 μm, J. Mol. Spectrosc. **93,** 179–195 (1982).
60. V. Malathy Devi, B. Fridovich, G.D. Jones, D.G.S. Snyder and A. Neuendorffer, *Temperature dependence of the widths of* N_2*-broadened lines of the* ν_3 *band of* $^{14}N^{16}O_2$, Appl. Opt. **21,** 1537–1538 (1982).

61. R.D. May and C.R. Webster, *Laboratory measurements of* NO_2 *line parameters near* 1600 cm^{-1} *for the interpretation of stratospheric spectra*, Geophys. Res. Let. **17,** 2157–2160 (1990).
62. S. Voigt, J. Orphal and J.P. Burrows, *The temperature and pressure dependence of the absorption cross sections of* NO_2 *in the* 250–800 nm *region measured by Fourier transform spectroscopy*, J. Photochemistry and Photobiology A (in press).
63. J.-M. Flaud, A. Perrin, J. Orphal, Quingli Kou, P.-M. Flaud, Z. Dutkiewicz and C. Piccolo, *New analysis of the* $\nu_5 + \nu_9 - \nu_9$ *hot band of* HNO_3, J. Quant. Spectrosc. Radiat. Transfer (in press, 2003).
64. R.A. Toth, L.R. Brown and E.A. Cohen, *Line strengths of nitric acid from* 850 *to* 920 cm^{-1}, J. Mol. Spectrosc. (in press, 2003).
65. A. Goldman, T.G. Kyle, and F.S. Bonomo, *Statistical band model parameters and integrated intensities for the* 5.9 micron, *and* 7.5 μm, *and* 11.3 μm *bands of* HNO_3 *vapour*, Appl. Opt. **10**, 65–73 (1971).
66. L.P. Giver, F.P.J. Valero, D. Goorvitch, and F.S. Bonomo, *Nitric-acid band intensities and band-model parameters from* 610 *to* 1760 cm^{-1}, J. Opt. Soc. Am. **B1**, 715–722 (1984).
67. S.T. Massie, A. Goldman, D.G. Murcray, and J.C. Gille, *Approximate absorption cross sections of* F12, F11, $ClONO_2$, N_2O_5, HNO_3, CCl_4, CF_4, F21, F113, F114, *and* HNO_4, Appl. Opt. **24**, 3426–3427 (1985).
68. J. Hjorth, G. Ottobrini, F. Cappellani, and G. Restelli, *A Fourier-transform infrared study of the rate-constant of the homogeneous gas-phase reaction* $N_2O_5 + H_2O$ *and determination of absolute infrared band intensities of* N_2O_5 *and* HNO_3, J. Phys. Chem. **91,** 1565–1568 (1987).
69. J.M. Flaud, M. Birk, G. Wagner, J. Orphal, J. Klee and W.J. Lafferty, *The far infrared spectrum of* HOCl: *line positions and intensities*, J. Mol. Spectrosc. **191**, 362–367 (1998).
70. J. Vander Auwera, J. Kleffmann, J.M. Flaud, G. Pawelke, H. Bürger, D. Hurtmans, and R. Petrisse, *Absolute* ν_2 *line intensities of* HOCl *by simultaneous measurements in the infrared and far infrared spectral regions*, J. Mol. Spectrosc. **204**, 36–47 (2000).
71. W. Thiel and J. Breidung, Private communication (2002).
72. L.R. Brown, Private communication (2002).
73. M.J. Hopper, J.W. Russell, and J. Overend, *Vibrational intensities of* CSF_2 *and* $CSCl_2$, Spectrochim. Acta **28A**, 1215–1218 (1972).
74. T.N. Adams, D.M. Weston, and R.A. Matulas, *Temperature dependence of spectral intensity of Fermi resonant* 1943 cm^{-1} *band of carbonyl fluoride*, J. Chem. Phys. **55**, 5674–5678 (1971).
75. R. Sams, Private communication.